Steps toward mapping the human vasculature by phage display

WADIH ARAP[1,2], MIKHAIL G. KOLONIN[1], MARTIN TREPEL[1], JOHANNA LAHDENRANTA[1], MARINA CARDÓ-VILA[1], RICARDO J. GIORDANO[1], PAUL J. MINTZ[1], PETER U. ARDELT[1], VIRGINIA J. YAO[1], CLAUDIA I. VIDAL[1], LIMOR CHEN[1], ANNE FLAMM[3], HELI VALTANEN[9], LISA M. WEAVIND[5], MARSHALL E. HICKS[6], RAPHAEL E. POLLOCK[7], GREGORY H. BOTZ[5], CORAZON D. BUCANA[2], ERKKI KOIVUNEN[9], DOLORES CAHILL[10], PATRICIA TRONCOSO[8], KEITH A. BAGGERLY[4], REBECCA D. PENTZ[3], KIM-ANH DO[4], CHRISTOPHER J. LOGOTHETIS[1] & RENATA PASQUALINI[1,2]

Departments of [1]Genito-Urinary Medical Oncology, [2]Cancer Biology, [3]Clinical Ethics, [4]Biostatistics, [5]Critical Care, [6]Diagnostic Radiology, [7]Surgical Oncology and [8]Pathology, The University of Texas M.D. Anderson Cancer Center, Houston, Texas, USA

[9]Department of Biosciences, Division of Biochemistry, University of Helsinki, Helsinki, Finland

[10]Max Planck Institute of Molecular Genetics, Berlin, Germany

M.G.K. and M.T. contributed equally to this study.

Correspondence should be addressed to W.A.; email: warap@notes.mdacc.tmc.edu, or R.P.; email: rpasqual@notes.mdacc.tmc.edu

The molecular diversity of receptors in human blood vessels remains largely unexplored. We developed a selection method in which peptides that home to specific vascular beds are identified after administration of a peptide library. Here we report the first *in vivo* screening of a peptide library in a patient. We surveyed 47,160 motifs that localized to different organs. This large-scale screening indicates that the tissue distribution of circulating peptides is nonrandom. High-throughput analysis of the motifs revealed similarities to ligands for differentially expressed cell-surface proteins, and a candidate ligand–receptor pair was validated. These data represent a step toward the construction of a molecular map of human vasculature and may have broad implications for the development of targeted therapies.

Despite major progress brought about by the Human Genome Project[1,2], the molecular diversity of blood vessels has just begun to be uncovered. Many therapeutic targets may be expressed in very restricted but highly specific and accessible locations in the vascular endothelium. Thus potential targets for intervention may be overlooked in high-throughput DNA sequencing or in gene arrays because these approaches do not generally take into account cellular location and anatomical and functional context.

We developed an *in vivo* selection method in which peptides that home to specific vascular beds are selected after intravenous administration of a phage-display random peptide library[3]. This strategy revealed a vascular address system that allows tissue-specific targeting of normal blood vessels[4,5] and angiogenesis-related targeting of tumor blood vessels[6–10]. Although the biological basis for such vascular heterogeneity remains unknown, several peptides selected by homing to blood vessels in mouse models have been used by several groups as carriers to guide the delivery of cytotoxic drugs[9], pro-apoptotic peptides[6], metalloprotease inhibitors[7], cytokines[11], fluorophores[12] and genes[13]. Generally, coupling to homing peptides yields targeted compounds that are more effective and less toxic than the parental compound[6,9,11]. Moreover, vascular receptors corresponding to the selected peptides have been identified in blood vessels of normal organs[14] and in tumor blood vessels[15,16]. Together, these results show that it is possible to develop therapeutic strategies based on selective expression of vascular receptors[17].

Although certain ligands and receptors isolated in mouse models have been useful to identify putative human homologs[10,15], it is unlikely that targeted delivery will always be achieved in humans using mouse-derived probes. Data from the Human Genome Project indicate that the higher complexity of the human species relative to other mammalian species derives from expression patterns of proteins at different tissue sites, levels or times rather from a greater number of genes[1,2]. In fact, several examples of species-specific differences in gene expression within the human vascular network have recently surfaced. The divergence in the expression patterns of the prostate-specific membrane antigen (PSMA) between human and mouse illustrates such species specificity. Selective expression of PSMA occurs in the human prostate, but not in the mouse prostate; instead, the mouse homolog of PSMA is expressed in the brain and kidney[18]. Additionally, PSMA is a marker of endothelial cells of tumor blood vessels in humans[19], whereas the mouse homolog of PSMA is undetectable in tumor-associated neovasculature in the mouse (W.D. Heston, pers. comm.). Another example of such divergence is the *TEM7* gene, which is highly expressed in a selective manner in the endothelium of human colorectal adenomas[20]. By contrast, mouse *Tem7* is expressed not in tumor blood vessels but in Purkinje cells instead[21]. Thus, striking species-specific differ-

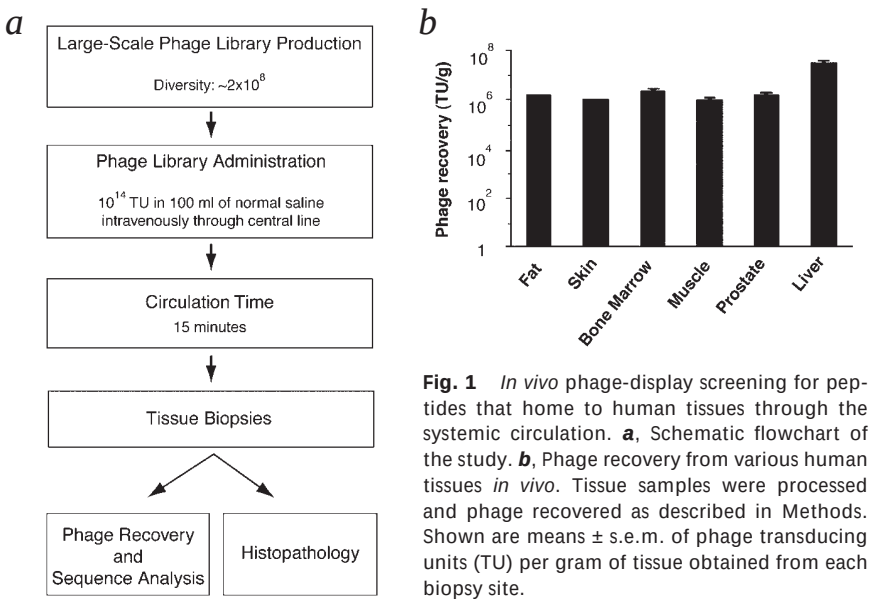

Fig. 1 *In vivo* phage-display screening for peptides that home to human tissues through the systemic circulation. ***a***, Schematic flowchart of the study. ***b***, Phage recovery from various human tissues *in vivo*. Tissue samples were processed and phage recovered as described in Methods. Shown are means ± s.e.m. of phage transducing units (TU) per gram of tissue obtained from each biopsy site.

ences in protein expression and ligand–receptor accessibility dictates that vascular targeting data obtained in animal models must be carefully evaluated before extrapolating to human studies.

Screening phage-display libraries in humans

We reasoned that *in vivo* selection of phage-display random peptide libraries in humans would advance the identification of human vascular targeting probes and facilitate development of targeted delivery of therapeutic and imaging agents to the vasculature. This study reports the initial step toward developing an *in vivo* phage display–based, ligand–receptor map of human blood vessels.

A large-scale preparation of a phage random peptide library containing the insert CX_7C (C, cysteine; X, any amino-acid residue) and designed to display a constrained cyclic loop within the pIII capsid protein was optimized to create the highest possible insert diversity[3]. The diversity of the library was approximately 2×10^8 and its final titer was approximately 1×10^{12} transducing units (TU) per ml.

A patient (see Methods) received an intravenous infusion of the unselected random phage library, and 15 min after infusion tissue biopsies were obtained to provide histopathological diagnosis and to recover phage from various organs (Fig. 1*a*).

Here we demonstrate the feasibility of producing phage-display random peptide libraries on a very large scale and of selecting phage clones that home to different human organs *in vivo* through the systemic circulation (Fig. 1*b*).

High-throughput analysis of selected peptides

To analyze the distribution of inserts from the random peptide library, we designed a high-throughput pattern recognition software to analyze short amino-acid residue sequences. This automated program allowed surveillance of peptide inserts recovered from the phage library screening.

Based on SAS (version 8; SAS Institute) and Perl (version 5.0), the program conducts an exhaustive amino-acid residue sequence count and keeps track of the relative frequencies of n distinct tripeptide motifs representing all possible n_3 overlapping tripeptide motifs in both directions ($n << n_3$). This analysis was applied for phage recovered from each target tissue and for the unselected CX_7C random phage-display peptide library. Counts were recorded for all overlapping interior tripeptide motifs, subject only to reflection and single-voting restrictions. No peptide was allowed to contribute more than once for a single tripeptide motif (or a reversed tripeptide motif). Tripeptide motifs in both directions are chemically nonsymmetrical and not necessarily equivalent. However, because we often recovered forward and reverse tripeptides recognizing the same receptor by *in vivo* phage display, we chose to take reflection into account, with the understanding that this is not a general feature that is applicable to every ligand–receptor pair interaction. Each peptide contributed five tripeptide motifs. Tripeptide motif counts were conditioned on the total number for all motifs being held fixed within a tissue. The significance of association of a given allocation of counts was assessed by the Fisher's exact test (one-tailed). Results were considered statistically significant at $P < 0.05$. In summary, to test for randomness of distribution, we compared the relative frequencies of a particular tripeptide motif from each target to those of the motifs from the unselected library; such an approach is intrinsically a large-scale contingency table association test.

Distribution of tripeptide motifs *in vivo*

To determine the distribution of the peptide inserts homing to specific sites after intravenous administration, we compared the relative frequencies of every tripeptide motif from each target tissue to those from the unselected library. We analyzed 4,716 phage inserts recovered from representative samples of five tissues (bone marrow, fat, skeletal muscle, prostate and skin) and from the unselected library. Tripeptide motifs were chosen for the phage insert analysis because three amino-acid residues seem to provide the minimal framework for structural formation and protein–protein interaction[22]. Examples of such biochemical recognition units and binding of ligand motifs to their receptors include RGD, LDV and LLG to integrins[23,24], NGR to aminopeptidase N/CD13 (refs 11,15) and GFE to membrane dipeptidase[4,14]. Each phage insert analyzed contained seven amino-acid residues and contributed five potential tripeptide motifs; thus, counting both peptide orientations, a total of 47,160 tripeptide motifs were surveyed.

Comparisons of the motif frequencies in a given organ relative to those frequencies in the unselected library demonstrate the nonrandom nature of the peptide distribution (Table 1); such a bias is particularly noteworthy given that only a single round of *in vivo* screening was performed. Of the tripeptide motifs selected from tissues, some were preferentially recovered in a single site whereas others were recovered from multiple sites. These data are consistent with some peptides homing in a tissue-specific manner and others targeting several tissues. We next adapted the ClustalW software from

the European Molecular Biology Laboratory[25] to analyze the original cyclic phage peptide inserts of seven amino-acid residues containing the tripeptide motifs. This analysis revealed four to six amino-acid residue motifs that were shared among multiple peptides isolated from a given organ (Fig. 2). We searched for each of these motifs in online databases (through the National Center for Biotechnology Information (NCBI; http://www.ncbi.nlm.nih.gov/BLAST/) and found that some appeared within known human proteins. Phage-display technology is suitable for targeting several classes of molecules (adhesion receptors, proteases, proteoglycans or growth factor receptors). Based on extensive work performed in murine models, the *in vivo* selection system seems to favor the isolation of peptides that recognize receptors that are selectively expressed in specific organs or tissues[17]. As our motifs are likely to represent sequences present in circulating ligands (either secreted proteins or surface receptors expressed on circulating cells) that home to vascular receptors, we compiled a panel of candidate human proteins potentially mimicked by selected peptide motifs (Table 2).

Table 1 Peptide motifs isolated by *in vivo* phage display screening

Target organ and motif	Motif frequency (%)	*P* value
Unselected library		
None	NA	NA
Bone marrow		
GGG*	2.3	0.0350
GFS*	1.0	0.0350
LWS*	1.0	0.0453
ARL	1.0	0.0453
FGG	1.1	0.0453
GVL	2.3	0.0137
SGT	1.1	0.0244
Fat		
EGG*	1.3	0.0400
LLV*	1.0	0.0269
LSP*	0.9	0.0402
EGR	1.1	0.0180
FGV	0.9	0.0402
Muscle		
LVS*	2.1	0.0036
GER	0.9	0.0036
Prostate		
AGG*	2.5	0.0340
EGR	1.0	0.0340
GER	0.9	0.0382
GVL	2.3	0.0079
Skin		
GRR*	2.9	0.0047
GGH*	0.9	0.0341
GTV*	0.8	0.0497
ARL	0.8	0.0497
FGG	1.3	0.0076
FGV	1.0	0.0234
SGT	1.0	0.0234

Peptide motifs isolated by *in vivo* phage display screening. Motifs occurring in peptides isolated from target organs but not from the unselected phage library (Fisher's exact test, one-tailed; $P < 0.05$). Number of peptide sequences analyzed per organ: unselected library, 446; bone marrow, 521; fat, 901; muscle, 850; prostate, 1,018; skin, 980. *, Motifs enriched only in a single tissue. Motif frequencies represent the prevalence of each tripeptide divided by the total number of tripeptides analyzed in the organ.

Validation of candidate ligands

It is tempting to speculate on a few biologically relevant homology hits. For example, a peptide contained within bone morphogenetic protein 3B (BMP-3B) was recovered from bone marrow. BMP-3B is a growth factor known to regulate bone development[26]. Thus, this protein may be mimicked by the isolated ligand homing to that tissue. We also isolated from the prostate a potential mimetope of interleukin 11 (IL-11), which has been previously shown to interact with receptors within endothelium and prostate epithelium[27,28]. In addition to secreted ligands, motifs were also found in several extracellular or transmembrane proteins that may operate selectively in the target tissue, such as sortilin in fat[29]. We have also recovered motifs from multiple organs; one such peptide is a candidate mimic peptide of perlecan, a protein known to maintain vascular homeostasis[30].

To test the tissue specificity of the peptides selected, we developed a phage-overlay assay for tissue sections. Because of the availability and well-characterized interaction between the candidate ligand (IL-11) and its receptor (IL-11Rα), we chose the motif RRAGGS, a peptide mimic of IL-11 (Table 2), for validation. We show by phage overlay on human tissue sections (see Methods) that a prostate-homing phage displaying an IL-11 peptide mimic specifically bound to the endothelium and to the epithelium of normal prostate (Fig. 3*a*), but not to control organs, such as skin (Fig. 3*b*). In contrast, a phage selected from the skin (displaying the motif HGGVG; Table 2), did not bind to prostate tissue (Fig. 3*c*); however, this phage specifically recognized blood vessels in the skin (Fig. 3*d*). Moreover, the immunostaining pattern obtained with an antibody against human IL-11Rα on normal prostate tissue (Fig. 3*e*) is undistinguishable from that of the CGRRAGGSC-displaying phage overlay (Fig. 3*a*); a control antibody showed no staining in prostate tissue (Fig. 3*f*). These findings were recapitulated in multiple tissue sections obtained from several different patients.

Finally, using a ligand–receptor binding assay *in vitro*, we demonstrate the interaction of the CGRRAGGSC-displaying phage with immobilized IL-11Rα at the protein–protein level (Fig. 4*a*). Such binding is specific because it was inhibited by the native IL-11 ligand in a concentration-dependent manner (Fig. 4*b*). Preliminary results indicate that serum IL-11 is elevated in a subset of prostate cancer patients (C.J.L., unpublished observations) and that the expression of IL-11Rα in tumors is upregulated in some cases of human prostate cancer (M.G.K., unpublished observations); these data may have clinical relevance.

Discussion

Aside from *in vivo* phage display, use of methods such as serial analysis of gene expression (SAGE) clearly shows that the genetic progression of malignant cells is paralleled by epigenetic changes in nonmalignant endothelial cells induced by angiogenesis of the tumor vasculature[20]. Because SAGE is based on differential expression levels of transcripts, it fails to address functional interactions (for example, binding) at the protein–protein level. The complexity of the human endothelium is also apparent from recent studies showing that the profile of certain endothelial cell receptors can vary depending on ethnic background[31]. In fact, *in vivo* phage-display in humans might reveal diversity of receptors expressed in the blood vessels even at the level of individual patients.

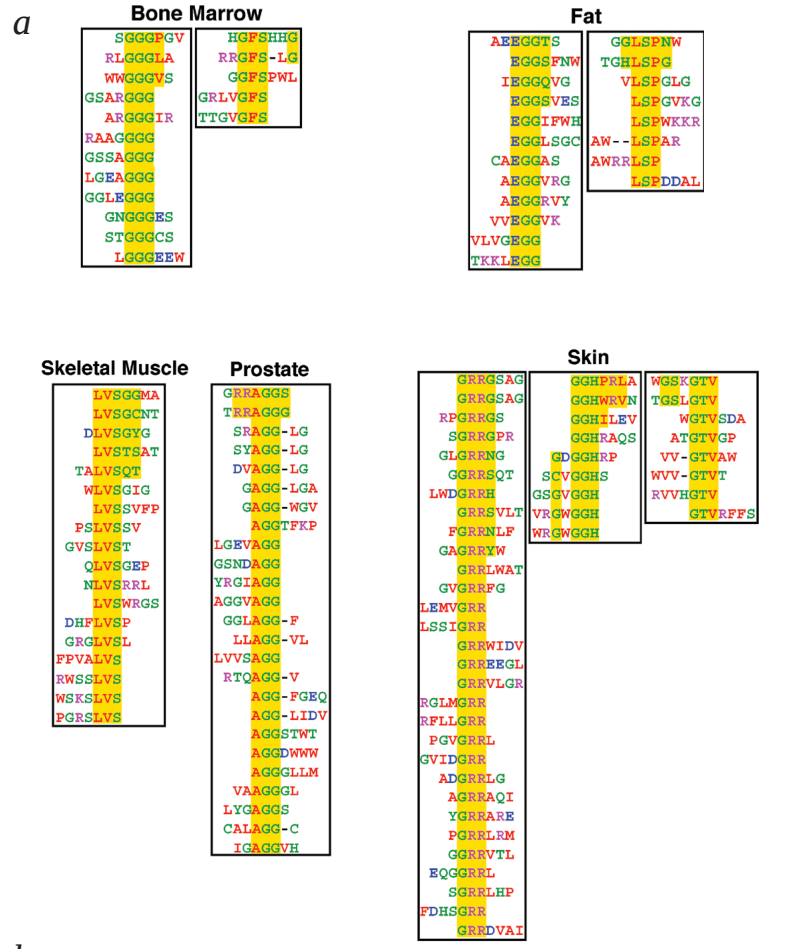

Fig. 2 Identification of extended homing motifs with the Clustal W program (European Molecular Biology Laboratory; EMBL). ***a*** and ***b***, Peptide sequences containing selected tripeptides (Table 1) preferentially isolated from each single tissue (*a*) or in multiple tissues (*b*) were aligned in clusters to obtain longer motifs shared between different peptides from each cluster. The software registers sequence identities and similarities among multiple peptide sequences and aligns the sequences by placing peptides with the most similarity or identity next to one another. Similarity between peptides at the level of amino-acid class is color-coded: red, hydrophobic; green, neutral and polar; pink, basic; blue, acidic. The original and extended peptide motifs are highlighted in yellow.

However, our validation studies show that at least some ligand–receptor pairs are detectable in multiple unrelated subjects. Another advantage of the method described here is that selected targeting peptides bind to native receptors as they are expressed *in vivo*. Even if a ligand–receptor interaction is mediated through a conformational rather than a linear epitope, it is possible to select binders in the screening. Furthermore, it is often difficult to ensure that proteins expressed in array systems maintain the correct structure and folding. Thus, peptides selected *in vivo* may be more suitable to clinical applications.

Precedent exists to suggest that phage can be safely administered to patients, as bacteriophage were used in humans during the pre-antibiotic era[32]. Ultimately, it may become possible to determine molecular profiles of blood vessels in specific conditions; infusing phage libraries systemically before resections of lung, prostate, breast and colorectal carcinomas, or even regionally before resection of limb sarcomas may yield useful vascular targets. Exploiting this experimental paradigm systematically with the analytical tools developed here may permit the construction of a molecular map outlining vascular diversity in each human organ, tissue or disease. Translation of high-throughput *in vivo* phage-display technology may provide a contextual and functional link between genomics and proteomics. Based on the therapeutic promise of peptide- or peptidomimetic-targeting probes[33], clinical applications are likely to follow.

Methods

Patient selection and clinical course. A 48-y-old male Caucasian patient was diagnosed with Waldenström macroglobulinemia (a B-cell malignancy) and previously treated by splenectomy, systemic chemotherapy (fludarabine, mitoxantrone and dexamethasone) and immunotherapy (anti-CD20 monoclonal antibody). In the few months preceding his admission, the disease became refractory to treatment and clinical progression with retroperitoneal lymphadenopathy, pancytopenia and marked bone marrow infiltration by tumor cells occurred. The patient was admitted with massive intracranial bleeding secondary to thrombocytopenia. Despite prompt craniotomy and surgical evacuation of a cerebral hematoma, the patient remained comatose with progressive and irreversible loss of brainstem function until the patient met the formal criteria for brain-based determination of death[34]; such determination was carried out by an independent clinical neurologist not involved in the project. Because of his advanced cancer, the patient was considered and rejected as transplant organ donor. After surrogate written informed consent was obtained from the legal next of kin, the patient was enrolled in the clinical study. Disconnection of the patient from life-support systems followed the pro-

Table 2 Examples of candidate human proteins mimicked by selected peptide motifs

Extended motif *	Human protein containing the motif	Protein description	Accession number
Bone marrow			
P**GGG**	Bone morphogenetic protein 3B	Growth factor, TGF-β family member	NP_004953
P**GGG**	Fibulin 3	Fibrillin- and EGF-like	Q12805
GHHSFG	Microsialin	Macrophage antigen, glycoprotein	NP_001242
Fat			
EGGT	LTBP-2	Fibrillin- and EGF-like, TGF-β Interactor	CAA86030
T**GGE**	Sortilin	Adipocyte differentiation-induced receptor	CAA66904
G**PSL**H	Protocadherin gamma C3	Cell adhesion	AAD43784
Muscle			
GG**SVL**	ICAM-1	Intercellular adhesion molecule	P05362
LVSGY	Flt4	Endothelial growth factor receptor	CAA48290
Prostate			
RR**AGG**S	Interleukin 11	Cytokine	NP_000632
RR**AGG**	Smad6	Smad family member	AAB94137
Skin			
GRRG	TGF-β1	Growth factor, TGF-β family member	XP_008912
HGG+G	Neuropilin-1	Endothelial growth factor receptor	AAF44344
+P**HGG**	Pentaxin	Infection/trauma-induced glycoprotein	CAA45158
P**HGG**	Macrophage-inhibitory cytokine-1	Growth factor, TGF-β family member	AAB88673
+P**HGG**	Desmoglein 2	Epithelial cell junction protein	S38673
VTG+SG	Desmoglein 1	Epidermal cell junction protein	AAC83817
Multiple organs			
EGRG	MMP-9	Gelatinase	AAH06093
G**RGE**	ESM-1	Endothelial cell-specific molecule	XP_003781
N**FGV**V	CDO	Surface glycoprotein, Ig- and fibronectin-like	NP_058648
GERIS	BPA1	Basement membrane protein	NP_001714
SI**REG**	Wnt-16	Glycoprotein	Q9UBV4
+**GVL**W	Sialoadhesin	Ig-like lectin	AAK00757
W**LVG**+	IL-5 receptor	Soluble interleukin 5 receptor	CAA44081
GGFR	Plectin 1	Endothelial focal junction-localized protein	CAA91196
GGFF	TRANCE	Cytokine, TNF family member	AAC51762
+S**GGF**	MEGF8	EGF-like protein	T00209
P**SGT**S	ICAM-4	Intercellular adhesion glycoprotein	Q14773
+**TGS**P	Perlecan	Vascular repair heparan sulfate proteoglycan	XP_001825

For similarity searches, tripeptide motif-containing peptides (in either orientation) selected by *in vivo* phage display screening were used. *Extended motifs containing at least 4–6 amino acid residues (Fig. 2) were analyzed using BLAST (NCBI) to search for similarity to known human proteins. Examples of candidate proteins potentially mimicked by the peptides selected in the *in vivo* screening are listed. Sequences correspond to the regions of 100% identity between the peptide selected and the candidate protein. Conserved amino acid substitutions are indicated as (+). Tripeptides shown in Table 1 are highlighted. TGF, transforming growth factor; TNF, tumor necrosis factor.

cedure. This study strictly adheres to current medical ethics recommendations and guidelines regarding human research[35], and it has been reviewed and approved by the Clinical Ethics Service, the Institutional Biohazard Committee, Clinical Research Committee and the Institutional Review Board of the University of Texas M.D. Anderson Cancer Center.

The University of Texas and researchers (W.A. and R.P.) have equity in NTTX Biotechnology, which is subjected to certain restrictions under university policy; the university manages the terms of these arrangements in accordance to its conflict-of-interest policies.

***In vivo* phage display.** Short-term intravenous infusion of the phage library (a total dose of 1×10^{14} phage TU suspended in 100 ml of saline) into the patient was followed by multiple representative tissue biopsies. Prostate and liver samples were obtained by needle biopsy under ultrasonographic guidance; skin, fat-tissue and skeletal-muscle samples were obtained by a surgical excision. Bone-marrow needle aspirates and core biopsy samples were also obtained. Histopathological diagnosis was determined by examination of frozen sections processed from tissues obtained at the bedside. Triplicate samples were processed for host bacterial infection, phage recovery and histopathological analysis. In brief, tissues were weighed, ground with a glass Dounce homogenizer, suspended in 1 ml of DMEM containing proteinase inhibitors (DMEM-prin; 1 mM phenylmethylsulfonyl fluoride (PMSF), 20 μg/ml aprotinin, and 1 μg/ml leupeptin), vortexed, and washed three times with DMEM-prin. Next, human tissue homogenates were incubated with 1 ml of host bacteria (log phase *Escherichia coli* K91kan; $OD_{600} \approx 2$). Aliquots of the bacterial culture were plated onto Luria–Bertani agar plates containing 40 μg/ml tetracycline and 100 μg/ml of kanamycin. Plates were incubated overnight at 37 °C. Bacterial colonies were processed for sequencing of phage inserts recovered from each tissue and from unselected phage library. Human samples were handled with universal blood and body fluid precautions.

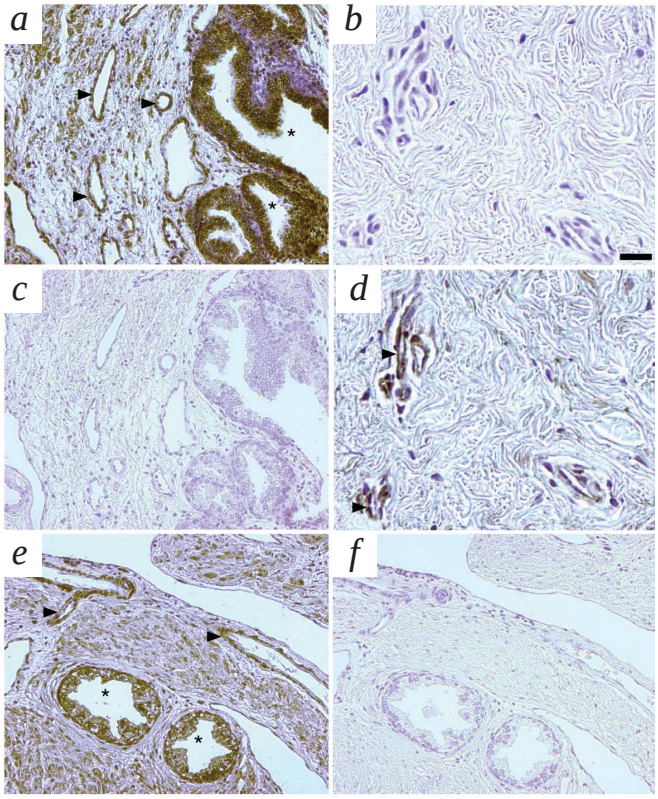

Fig. 3 Validation of the candidate receptor–ligand pairs resulting from the *in vivo* selection. ***a*–*f***, Phage clones isolated from prostate and from skin were evaluated for binding to human tissues in an overlay assay. Shown are paraffin-embedded tissue sections of human prostate (*a*, *c*, *e* and *f*) and of human skin (*b* and *d*) overlaid with prostate-homing CGRRAGGSC-displaying phage (*a* and *b*) or skin-homing CHGGVGSGC-displaying phage (*c* and *d*). Phage were detected by using an anti-M13 phage antibody. In *e*, IL-11Rα expression was determined by conventional immunostaining with an anti-IL-11Rα antibody; *a* and *e* show similar immunostaining patterns (brown staining). *f*, Negative control antibody on prostate tissue sections. Arrowheads, positive endothelium; asterisks, positive epithelium. Scale bar, 160 μm (*a*, *c*, *e* and *f*); 40 μm (*b* and *d*).

Statistical analysis. Let p be the probability of observing a particular tripeptide motif under total randomness, and $q = 1 - p$. Under such parameters, the probability of observing K sequences characterized as a particular tripeptide motif out of n_3 total tripeptide motif sequences is binomial (n_3, p) and may be approximated by the equation $p_K = \Phi[(k + 1)/sqrt(n_3\, pq)] - \Phi[k/sqrt(n_3\, pq)]$, where Φ is the usual cumulative Gaussian probability. The value p_K may be treated as a P value in testing for total randomness of observing exactly K sequences of a particular tripeptide motif. However, this test requires exact knowledge of the true value of p, which it is difficult to obtain in practice with certainty. Therefore, to identify the motifs that were isolated in the screening, the count for each tripeptide motif within each tissue was compared with the count for that tripeptide motif within the unselected library.

Immunocytochemistry and phage overlays. Immunohistochemistry on sections of fixed human paraffin-embedded tissues was done using the LSAB+ peroxidase kit (DAKO, Carpinteria, California) as described[3]. For overlay experiments, phage was used at the concentration of 5×10^{10} TU/ml. For phage immunolocalization, a rabbit anti-fd bacteriophage antibody (B-7786; Sigma) was used at 1:500 dilution. For IL-11Rα immunolocalization, a goat antibody (sc-1947; Santa Cruz Biotechnology, Santa Cruz, California) was used at 1:10 dilution. Phage binding to tissue sections was evaluated by the intensity of immunostaining relative to controls.

***In vitro* protein binding assays.** Recombinant (R&D Systems, Minneapolis, Minnesota) interleukin-11 receptor α (IL-11Rα), vascular endothelial growth factor receptor-1 (VEGFR1), and leptin receptor (OB-R) were immobilized on microtiter wells (at 1 μg in 50 μl PBS) overnight at 4°C, washed twice with PBS, blocked with 3% BSA in PBS for 2 h at room temperature, and incubated with 1x 10^9 TU of CGRRAGGSC-displaying phage in 50 μl of 1.5% BSA in PBS. An unrelated phage clone (displaying the peptide CRVDFSKGC) and insertless phage (fd-tet) were used as controls. After 1 h at room temperature, wells were washed nine times with PBS, after which bound phage were recovered by bacterial infection and plated as described[3]. Either IL-11 or IL-1 (negative control) was used to inhibit phage binding to IL-11Rα. Phage were incubated with the immobilized IL-11Rα in the presence of increasing concentrations of either IL-11 or IL-1. Binding of CGRRAGGSC-displaying phage on immobilized IL-11Rα in the absence of interleukins was set to 100%.

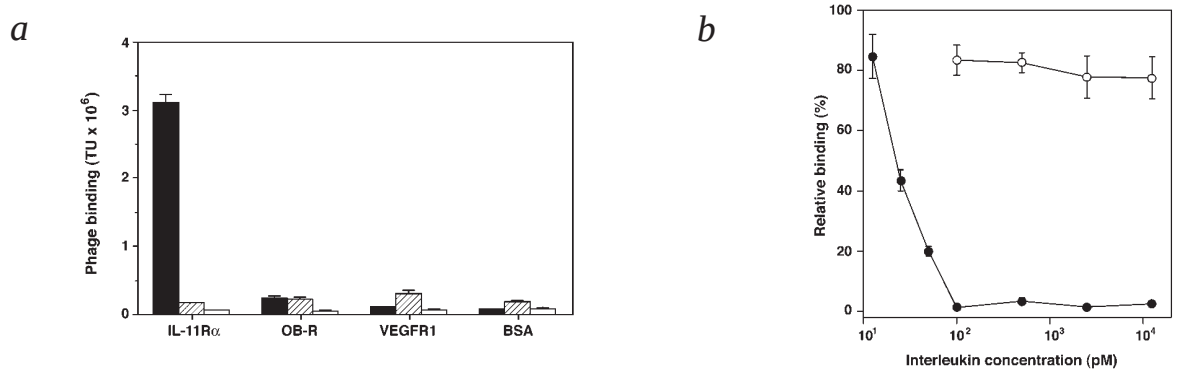

Fig. 4 Characterization of CGRRAGGSC-displaying phage binding properties by using purified receptors *in vitro*. ***a***, Recombinant interleukin-11 receptor α (IL-11Rα), vascular endothelial growth factor receptor-1 (VEGFR1), or leptin receptor (OB-R) were incubated with the CGRRAGGSC -displaying phage (■). VEGFR1 was used as a representative vascular receptor; OB-R was used because it is homologous to a coreceptor of IL-11Rα. An unrelated phage clone (displaying the peptide CRVDFSKGC, ▨) and insertless phage (fd-tet, □) were used as controls. Phage binding was evaluated and quantified as described (see Methods). ***b***, Specificity of phage binding to the IL-11 receptor. Phage were incubated with the immobilized IL-11Rα in the presence of increasing concentrations of either IL-11 (native ligand, ●) or IL-1 (negative control, ○). The experiments were performed three times with similar results. Shown are mean ± s.e.m. from triplicate wells.

Acknowledgements

We thank R.C. Bast, Jr., R.R. Brentani, W.K. Cavenee, A.C. von Eschenbach, I.J. Fidler, W.K. Hong, D.M. McDonald, J. Mendelsohn and L.A. Zwelling for comments on the manuscript; W.D. Heston for sharing unpublished data; C.L. Cavazos, P.Y. Dieringer, R.G. Nikolova, C.A. Perez, B.H. Restel, C.P. Soto and X. Wang for technical assistance. This work was funded in part by grants from NIH (CA90270 and CA8297601 to R.P., CA90270 and CA9081001 to W.A.) and awards from the Gilson–Longenbaugh Foundation and CaP CURE (to R.P. and W.A.). M.G.K., J.L. and P.J.M. received support from the Susan G. Komen Breast Cancer Foundation, R.J.G. from FAPESP (Brazil), M.C.V. from the Department of Defense, L.C. from the NCCRA and E.K. from the Academy of Finland.

Competing interests statement

The authors declare competing financial interests; see the Nature Medicine *web site (http://medicine.nature.com) for details.*

RECEIVED 19 NOVEMBER 2001; ACCEPTED 2 JANUARY 2002

1. Lander, E.S. *et al.* Initial sequencing and analysis of the human genome. *Nature* **409**, 860–921 (2001).
2. Venter, J.C. *et al.* The sequence of the human genome. *Science* **291**, 1304–1351 (2001).
3. Pasqualini, R., Arap, W., Rajotte, D. & Ruoslahti, E. *In vivo* phage display. In *Phage display: a laboratory manual.* (eds. Barbas, C. F., Burton, D.R., Scott, J.K. & Silverman, G.J.) 1–24 (Cold Spring Harbor Laboratory Press, Cold Spring Harbor, New York, 2000).
4. Rajotte, D. *et al.* Molecular heterogeneity of the vascular endothelium revealed by *in vivo* phage display. *J. Clin. Invest.* **102**, 430–437 (1998).
5. Pasqualini, R. & Ruoslahti, E. Organ targeting *in vivo* using phage display peptide libraries. *Nature* **380**, 364–366 (1996).
6. Ellerby, H.M. *et al.* Anti-cancer activity of targeted pro-apoptotic peptides. *Nature Med.* **5**, 1032–1038 (1999).
7. Koivunen, E. *et al.* Tumor targeting with a selective gelatinase inhibitor. *Nature Biotechnol.* **17**, 768–774 (1999).
8. Burg, M.A., Pasqualini, R., Arap, W., Ruoslahti, E. & Stallcup, W.B. NG2 proteoglycan-binding peptides target tumor neovasculature. *Cancer Res.* **59**, 2869–2874 (1999).
9. Arap, W., Pasqualini, R. & Ruoslahti, E. Cancer treatment by targeted drug delivery to tumor vasculature in a mouse model. *Science* **279**, 377–380 (1998).
10. Pasqualini, R., Koivunen, E. & Ruoslahti, E. α_v integrins as receptors for tumor targeting by circulating ligands. *Nature Biotechnol.* **15**, 542–546 (1997).
11. Curnis, F. *et al.* Enhancement of tumor necrosis factor α antitumor immunotherapeutic properties by targeted delivery to aminopeptidase N (CD13). *Nature Biotechnol.* **18**, 1185–1190 (2000).
12. Hong, F. D. & Clayman, G. L. Isolation of a peptide for targeted drug delivery into human head and neck solid tumors. *Cancer Res.* **60**, 6551–6556 (2000).
13. Trepel, M., Grifman, M., Weitzman, M.D. & Pasqualini, R. Molecular adaptors for vascular-targeted adenoviral gene delivery. *Hum. Gene Ther.* **11**, 1971–1981 (2000).
14. Rajotte, D. & Ruoslahti, E. Membrane dipeptidase is the receptor for a lung-targeting peptide identified by *in vivo* phage display. *J. Biol. Chem.* **274**, 11593–11598 (1999).
15. Pasqualini, R. *et al.* Aminopeptidase N is a receptor for tumor-homing peptides and a target for inhibiting angiogenesis. *Cancer Res.* **60**, 722–727 (2000).
16. Bhagwat, S.V. *et al.* CD13/APN is activated by angiogenic signals and is essential for capillary tube formation. *Blood* **97**, 652–659 (2001).
17. Kolonin, M.G., Pasqualini, R. & Arap, W. Molecular addresses in blood vessels as targets for therapy. *Curr. Opinion. Chem. Biol.* ***5***, 308–313 (2001).
18. Bacich, D.J., Pinto, J.T., Tong, W.P. & Heston, W.D. Cloning, expression, genomic localization, and enzymatic activities of the mouse homolog of prostate-specific membrane antigen/NAALADase/folate hydrolase. *Mamm. Genome* **12**, 117–123 (2001).
19. Chang, S.S. *et al.* Five different anti-prostate-specific membrane antigen (PSMA) antibodies confirm PSMA expression in tumor-associated neovasculature. *Cancer Res.* **59**, 3192–3198 (1999).
20. St Croix, B. *et al.* Genes expressed in human tumor endothelium. *Science* **289**, 1197–1202 (2000).
21. Carson-Walter, E.B. *et al.* Cell surface tumor endothelial markers are conserved in mice and humans. *Cancer Res.* **61**, 6649–6655 (2001).
22. Vendruscolo, M., Paci, E., Dobson, C.M. & Karplus, M. Three key residues form a critical contact network in a protein folding transition state. *Nature* **409**, 641–645 (2001).
23. Ruoslahti, E. RGD and other recognition sequences for integrins. *Annu. Rev. Cell Dev. Biol.* **12**, 697–715 (1996).
24. Koivunen, E. *et al.* Inhibition of β_2 integrin-mediated leukocyte cell adhesion by leucine-leucine-glycine motif-containing peptides. *J. Cell Biol.* **153**, 905–916 (2001).
25. Thompson, J.D., Higgins, D.G. & Gibson, T.J. CLUSTAL W: improving the sensitivity of progressive multiple sequence alignment through sequence weighting, position-specific gap penalties and weight matrix choice. *Nucleic Acids Res.* **22**, 4673–4680 (1994).
26. Daluiski, A. *et al.* Bone morphogenetic protein-3 is a negative regulator of bone density. *Nature Genet.* **27**, 84–88 (2001).
27. Mahboubi, K., Biedermann, B.C., Carroll, J.M. & Pober, J.S. IL-11 activates human endothelial cells to resist immune-mediated injury. *J. Immunol.* **164**, 3837–3846 (2000).
28. Campbell, C.L., Jiang, Z., Savarese, D.M. & Savarese, T.M. Increased expression of the interleukin-11 receptor and evidence of STAT3 activation in prostate carcinoma. *Am. J. Pathol.* **158**, 25–32 (2001).
29. Lin, B.Z., Pilch, P.F. & Kandror, K.V. Sortilin is a major protein component of Glut4-containing vesicles. *J. Biol. Chem.* **272**, 24145–24147 (1997).
30. Nugent, M.A., Nugent, H.M., Iozzo, R.V., Sanchack, K. & Edelman, E.R. Perlecan is required to inhibit thrombosis after deep vascular injury and contributes to endothelial cell-mediated inhibition of intimal hyperplasia. *Proc. Natl Acad. Sci. USA* **97**, 6722–6727 (2000).
31. Wu, K.K. *et al.* Thrombomodulin Ala455Val polymorphism and risk of coronary heart disease. *Circulation* **103**, 1386–1389 (2001).
32. Barrow, P.A. & Soothill, J. S. Bacteriophage therapy and prophylaxis: rediscovery and renewed assessment of potential. *Trends Microbiol.* **5**, 268–271 (1997).
33. Latham, P.W. Therapeutic peptides revisited. *Nature Biotechnol.* **17,** 755–757 (1999).
34. Wijdicks, E.F. The diagnosis of brain death. *N. Engl. J. Med.* **344**, 1215–1221 (2001).
35. Implementing Human Research Regulations; in *President's Commission for the Study of Ethical Problems in Medicine and Biomedical and Behavioral Research.* (The United States of America Government's Printing Office, Washington, DC; 1983).